MFCIWP(87)/P49

CLM-R276

# Some Calculations of Shocks and Detonations for Gas Mixtures

D. F. Fletcher and A. Thyagaraja

Culham Laboratory, Abingdon, Oxon. OX14 3DB

ABSTRACT

In this paper we report on a computer code (CULDESAC) developed to model the flow of a mixture of two gases. This is the first stage in the development of a code for modelling the detonation stage of vapour explosions. We describe the equations governing this situation and the numerical scheme developed to solve them. Calculations are presented for a steady-state shock, transient simulations of shock tubes (in one case containing different gases in each section) and detonations. We conclude that the numerical scheme presented in this paper is suitable for the simulation of compressible flows encountered in the detonation stage of vapour explosions.

March 1987.

Culham Laboratory
United Kingdom Atomic Energy Authority
Abingdon
Oxfordshire OX14 3DB

March 1987

ISBN: 085311 1596
Price: £5.00
Available from H.M. Stationery Office

Contents

## NOMENCLATURE

| | |
|---|---|
| $c$ | speed of sound |
| $c_v$ | specific heat at constant volume |
| $e$ | internal energy |
| $h$ | enthalpy |
| $K$ | constant in momentum equilibration term |
| $p$ | pressure |
| $R$ | constant in temperature equilibration term |
| $T$ | temperature |
| $t$ | time |
| $v$ | velocity |
| $x$ | space coordinate |

### Greek symbols

| | |
|---|---|
| $\rho$ | density |
| $\lambda$ | constant in drag work term |
| $\gamma$ | ratio of specific heats |
| $\tau_D$ | drag relaxation time |
| $\tau_T$ | temperature relaxation time |

### Subscripts

| | |
|---|---|
| 1,2 | Gases 1 and 2 |
| i | notation for either gas |
| s | stagnation |

## 1. Introduction

If a hot liquid (melt) is brought into contact with a cooler volatile liquid (coolant) in some circumstances the coolant may be vaporised so rapidly and coherently that an explosion results. Such explosions are known variously as steam explosions, vapour explosions or Molten Fuel Coolant Interactions. They are of concern in the metal-casting industry [1] and in the transportation of liquefied Natural Gas (LNG) over water [2]. They are postulated to occur in submarine volcanisms [3] and are studied in connection with nuclear reactor safety [4].

A large scale interaction involving melt and water is known to require a well-defined sequence of events. Firstly, the melt and coolant must mix together on a coarse scale with melt and coolant zones having a typical dimension of 10mm. During this stage the melt is surrounded by a vapour blanket so that heat transfer is relatively slow and there is little pressure generation. If the vapour blanket collapses locally in some region of the mixture this leads to high heat transfer rates and fragmentation of the melt. This in turn leads to a rapid increase in pressure locally. In some circumstances this pressure disturbance could propagate as a detonation wave leading to fine fragmentation of the melt and coherent energy transfer to the coolant. The high pressure coolant can then expand causing damage due to the high pressures or the impact of material flowing away from the interaction zone.

Previous work by the present authors has concentrated on the study of the coarse mixing stage. This necessitated the development of a two-dimensional transient three-component (melt, water and steam) incompressible multiphase flow code. The model and its validation is described in references 5 - 11. The model of coarse mixing allows the volume fractions and the melt length-scale to be calculated as a function of time. Thus it can be used to determine the effect of varying external parameters, such as ambient pressure, on mixing. The next stage in the

modelling of the vapour explosion phenomenon is to determine which mixture configurations can support the escalation of localised interactions into propagating detonations. Thus we intend to develop a multiphase flow code to determine the behaviour of a prescribed pressure pulse applied to a given mixture. This will allow us to determine which mixtures can be detonated and which cannot because, for example, there is too much steam or the melt fragments are too large.

Our previous modelling work was concerned with incompressible multiphase flow. Clearly the extension to the detonation case requires the development of a computer code which can model compressible transient multi-component flow. As in our previous work we intend to develop this model in a number of stages. In this paper we describe the first stage - a code (called CULDESAC) developed to model the flow of two gases. This has enabled us to examine the accuracy and stability of our proposed solution scheme and to gain experience in computing shock waves and detonations.

In section 2 we describe the equations to be solved together with the necessary boundary and initial conditions. In section 3 the solution procedure is described. In section 4 we present some calculations of flows involving shock waves and expansion fans. In section 5 we examine the theory of detonations in gases and present some numerical simulations. Finally, in section 6 we draw some conclusions on this first phase of model development.

## 2. Mathematical Formulation

In this section we present the equations governing the behaviour of a mixture of gases. We restrict our attention to a one dimensional duct with a constant cross-sectional area. The governing equations are:

$$\frac{\partial}{\partial t} \rho_1 + \frac{\partial}{\partial x} (\rho_1 v_1) = 0 \qquad (1)$$

$$\frac{\partial}{\partial t} \rho_2 + \frac{\partial}{\partial x} (\rho_2 v_2) = 0 \qquad (2)$$

$$\frac{\partial}{\partial t}(\rho_1 v_1) + \frac{\partial}{\partial x}(\rho_1 v_1^2) = -\frac{\partial p_1}{\partial x} + K(v_2 - v_1) \tag{3}$$

$$\frac{\partial}{\partial t}(\rho_2 v_2) + \frac{\partial}{\partial x}(\rho_2 v_2^2) = -\frac{\partial p_2}{\partial x} + K(v_1 - v_2) \tag{4}$$

$$\frac{\partial}{\partial t}(\rho_1(e_1 + 1/2\, v_1^2)) + \frac{\partial}{\partial x}(\rho_1 v_1(h_1 + 1/2\, v_1^2)) =$$

$$v_1 K(v_2 - v_1) + \lambda K(v_2 - v_1)^2 + R(T_2 - T_1) \tag{5}$$

$$\frac{\partial}{\partial t}(\rho_2 (e_2 + 1/2\, v_2^2)) + \frac{\partial}{\partial x}(\rho_2 v_2(h_2 + 1/2\, v_2^2)) =$$

$$v_2 K(v_1 - v_2) + (1 - \lambda) K(v_2 - v_1)^2 + R(T_1 - T_2) \tag{6}$$

The above equations describe conservation of mass, momentum and total energy for each of the gas species 1 and 2. At this stage we will make some observations about this system of equations which will prove useful later.

(i) All the equations are hyperbolic so there is no problem of "ill-posedness" as occurs in the multiphase flow formulation [12].

(ii) Equations (1) and (2) represent conservation of mass and we have assumed that there are no internal sources or sinks in the solution domain.

(iii) Equations (3) and (4) represent conservation of momentum for each species. Note that each species only feels a pressure from its own species (c.f. Dalton's law of partial pressure [13]) and the total pressure is given by

$$p = p_1 + p_2 \tag{7}$$

(iv) We have ignored viscous terms. Since the flow is one dimensional there are no shear forces and compression (or bulk) viscosity forces are known to be small in most normal situations [14].

(v) The terms $K(v_2 - v_1)$ and $K(v_1 - v_2)$ model drag between the species. The chosen form ensures that Newton's third law is automatically satisfied for any choice of K. There appears to be no general theory available to describe inter-species drag, so that for the purposes of the present paper we have made the following assumption

$$K = \frac{\rho_1 \rho_2}{(\rho_1 + \rho_2)\ \tau_D} \tag{8}$$

Equation (8) ensures that the drag is equal to zero if either species is absent and $\tau_D$ is a user-specified relaxation time.

(vi) Equations (5) and (6) represent conservation of stagnation energy. These equations were formed by adding the mechanical energy equations (e.g. equation 3 multiplied by $v_1$) to the thermodynamic energy equation. Note that the time derivative acts on $e + 1/2\ v^2$ but the convective term contains $h + 1/2\ v^2$, where

$$h = e + \frac{p}{\rho} \tag{9}$$

(vii) The terms involving K on the r.h.s. of equations (5) and (6) are due to drag work. Their form ensures that the total energy of a closed system is conserved. The parameter $\lambda$ takes values between 0 - 1 and is otherwise arbitrary [15]. In all cases we have assumed $\lambda = 0.5$.

(viii) The terms $R(T_2 - T_1)$ and $R(T_1 - T_2)$ represent thermal equilibration between the species. Again there is no general theory available to determine R and we have chosen for the present calculations to use the form

$$R = \frac{\rho_1 \rho_2 c_{v1} c_{v2}}{(\rho_1 c_{v1} + \rho_2 c_{v2})\ \tau_T} \tag{10}$$

where $\tau_T$ is a suitable relaxation time.

In addition to the above equations, an equation of state and a caloric equation are needed for each species. We have chosen to use ideal gases so that

$$p_i = (\gamma_i - 1)\, c_{vi} \rho_i T_i \tag{11}$$

and

$$e_i = c_{vi} T_i \tag{12}$$

where $c_v$ is the specific heat capacity at constant volume and $\gamma$ is the ratio of specific heats.

## 2.1 Initial and Boundary Conditions

In the present work we have solved the above equations for two different types of problems.

Firstly, we have used the model to obtain steady state solutions for shock waves and detonations. In this situation all the variables are specified at the inlet (i.e. p, $\rho$, T and v) and the exit pressure is specified. This is sufficient to determine the solution uniquely. Any suitable initial condition can be used and the chosen initial condition determines only the location of the shock.

Secondly, we have used the code to examine initial value problems. For example the code has been used to examine the flow of gases in a shock tube. In this case initial conditions on p, $\rho$, T and v are specified and suitable boundary conditions at the end of the tube are needed. In our calculations we assume that the tube is closed at both ends so that the velocity is set to zero. No other boundary conditions are needed.

## 3. Solution Procedure

A vast literature exists on the solution of the inviscid Euler equations (the single component form of the present equations). The need for accurate and robust schemes to solve these equations is due to their importance in the aircraft industry. An excellent review of these schemes and the philosophy behind them is given by Moretti [16]. For the present purpose we will make a few general observations.

Numerical schemes can be split up broadly into two types: "shock fitting" and "shock capturing". In "shock fitting" schemes the differential equations are solved in the regions of continuous flow and these regions are joined by using the Rankine-Hugoniot equations, hence the term "shock fitting". In "shock capturing" schemes the equations are solved throughout the solution domain and the location of shocks is predicted by the scheme. For these schemes to work the equations must be written in conservation form so that they contain the shock conditions. It is this latter type of scheme which is of interest to us since we will not know the shock position a priori; its position will depend on how efficiently the detonation progresses.

The literature contains numerous novel techniques which attempt to exploit the features of hyperbolic systems (in particular the existence of real characteristics) to produce high order accurate schemes. These schemes are often very complex and it is not clear how they would generalise to a "common pressure" multiphase flow formulation. For this reason we have decided to try the simplest first-order accurate scheme and to see how well it predicts flows similar to those of interest in the multiphase detonation problem.

If we use a first order accurate scheme for convective terms (i.e. upstream differencing) the scheme will provide sufficient "numerical viscosity" to capture the shock and ensure that there are no oscillations in pressure downstream of any shocks. This is important as in the ultimate situation of interest the downstream pressure and flow velocities

will determine the melt fragmentation rate which in turn determines the amount of energy fed into the system.

## 3.1 Description of the Scheme Used

The partial differential equations described in section 2 were solved using a finite difference method. A staggered grid was used with $\rho$, p and T being stored at the cell centres and velocities being stored at the cell boundaries. This is illustrated in Figure 1. All convective terms were upstream differenced. The solution procedure will be outlined below.

(i) Time advance the density equations using an explicit method. The differencing was carried out as follows:

$$\rho_i^{n+1} = \rho_i^n + \frac{\Delta t}{\Delta x}\left[F_{i-1}^n - F_i^n\right] \qquad (13)$$

where $F_{i-1}^n = v_{i-1}^n \rho_-^n$

$$F_i^n = v_i^n \rho_+^n$$

$$\rho_-^n = \rho_{i-1}^n \quad \text{if} \quad v_{i-1}^n \geqslant 0$$

$$= \rho_i^n \quad \text{if} \quad v_{i-1}^n < 0$$

$$\rho_+^n = \rho_i^n \quad \text{if} \quad v_i^n \geqslant 0$$

$$= \rho_{i+1}^n \quad \text{if} \quad v_i^n < 0$$

Using results from a previous paper [7] we know that the above scheme will always produce non-negative densities and that the mass of each species will always be conserved in a closed system. The above scheme is stable provided

$$\max_{1 \leqslant i \leqslant N} \frac{(c+|v_i|)\Delta t}{\Delta x} < 1 \qquad (14)$$

(ii) The next stage is to solve for the velocities. We use a completely explicit scheme. The pressure gradient terms are evaluated at the old time. The convective terms $\rho v^2$ are differenced as $(\rho v)^n v^{n+1/2}$ i.e. the mid-time velocity is transported by the mass flux evaluated at the old time. This practice ensures that the Rankine-Hugoniot condition can be satisfied for a steady shock, as in this case the same flux is used to transport density, velocity and energy. The new velocities are evaluated at the mid time for accuracy. Due to the convective term the new velocities are linked to their nearest neighbours and a tri-diagonal (TDMA) solver is used to determine the new velocity field simultaneously throughout the solution domain.

The finite difference form of the momentum equation for gas 1 is given by

$$(\rho_{1i+1/2} v_{1i})^{n+1} - (\rho_{1i+1/2} v_{1i})^n = A_i^+ v_{1i+1}^{n+1/2} + A_i^0 v_{1i}^{n+1/2} + A_i^- v_{1i-1}^{n+1/2}$$

$$- \frac{\Delta t}{\Delta x} (p_{i+1}^n - p_i^n) + \Delta t \, K_i^n (v_{2i}^n - v_{1i}^n) \qquad (15)$$

where

$$A_i^+ = - \frac{\Delta t}{\Delta x} F_{i+\frac{1}{2}}^n (1-\theta_i^+)$$

$$A_i^- = \frac{\Delta t}{\Delta x} F_{i-\frac{1}{2}}^n \theta_i^- \qquad (16)$$

$$A_i^0 = \frac{\Delta t}{\Delta x} F_{i+\frac{1}{2}}^n (1-\theta_i^-) - \frac{\Delta t}{\Delta x} F_{i-\frac{1}{2}}^n \theta_i^+$$

and the mass fluxes are given by

$$F_{i+\frac{1}{2}}^n = 1/2(F_i^n + F_{i+1}^n)$$

$$F_{i-\frac{1}{2}}^n = 1/2(F_{i-1}^n + F_i^n) \qquad (17)$$

where:

$$\theta_i^+ = 1 \quad \text{if} \quad F^n_{i+\frac{1}{2}} > 0$$

$$= 0 \quad \text{if} \quad F^n_{i+\frac{1}{2}} \leq 0 \qquad (18)$$

$$\theta_i^- = 1 \quad \text{if} \quad F^n_{i-\frac{1}{2}} > 0 \qquad (19)$$

$$= 0 \quad \text{if} \quad F^n_{i-\frac{1}{2}} \leq 0$$

$$\rho^n_{i+1/2} = (\rho^n_i + \rho^n_{i+1})/2 \qquad (20)$$

$$v_i^{n+1/2} = (v_i^{n+1} + v_i^n)/2 \qquad (21)$$

In the solution scheme the usual principles of reciprocity are used i.e.

$$\theta^-_{i+1} = \theta^+_i \qquad (22)$$

The above scheme was found to work well and to lead to very little smearing of shock fronts. In an early version of the code we obtained cell face mass fluxes from the product of the density stored at the face and the average of the velocity stored each side of the face (i.e. $F^n_{i+\frac{1}{2}} = \rho_{i+1}(v_{i+1} + v_i)/2$). This was found to be very diffusive and did not satisfy the Rankine-Hugoniot equations in their finite difference form.

(iii) The energy equations (5) and (6) were solved using the same method as that used for the density equations. The solution variable is $\rho(e + 1/2v^2) = \rho e_s$. Thus exactly the same scheme as equation (13) was used to determine $(\rho e_s)^{n+1}$ noting that the flux term applies to the stagnation enthalpy. The source terms arising from drag work and temperature equilibration were evaluated at the old time. Because the

scheme uses a staggered grid, v and e are not stored at the same locations, and it was necessary to define

$$e_{si} = e_i + 1/2\ v_{i-1}^2 \bar{\theta}_i + 1/2\ v_i^2 (1-\bar{\theta}_i) \qquad (23)$$

With the definition it is a simple matter to determine e given $e_s$ since the velocity field is time advanced before the solution of the energy equation.

Given the new energy field new temperature and pressure fields were determined using equations (12) and (11) respectively.

## 4. Test Problems

The code was used to examine two test problems. One was the steady-state solution of a shock wave given the upstream conditions and the pressure jump across the shock. The other was a transient problem, the modelling of flow in a shock tube.

### 4.1 Stationary Shock

This problem allows us to determine how accurately the code can predict a shock and to determine by how much the scheme 'smears' shocks. The parameters used in the calculation are given in Table 1. This problem only involves one gas. The conditions for the second gas were set equal to the upstream conditions of the gas used in the simulation and all coupling terms ($1/\tau_D$ and $1/\tau_T$) were set to zero.

Figures 2(a) - 2(e) show plots of the pressure, density, temperature, Mach number and entropy for a simulation using 72 grid points. These plots show that changes in quantities across the shock are not excessively smeared and that the changes in density, temperature, velocity and entropy are very accurately predicted. This is because the Rankine-Hugoniot equations are built into the steady-state finite difference form of the conservation equations. The entropy rise is monotonic and there is no over-shoot in the entropy at the shock front. This is an important internal consistency check, since, unlike the Rankine conditions, the entropy equation is not solved in the scheme. The entropy

of the gas is calculated from $\rho$ and T after the solution is completed. Thus we have produced a thermodynamically consistent scheme [17] without using any particularly complicated practices. It is of interest to note that the practice embodied in Equation (17) played a decisive role in obtaining a monotonic (i.e. thermodynamically consistent) entropy profile.

## 4.2. Shock Tube

Consider a tube closed at both ends and divided part way down its length by a diaphragm. One section is filled with high pressure gas and the other a low pressure gas (not necessarily the same gas as in the high pressure section) and the diaphragm is then ruptured. This results in a shock wave travelling into the low pressure gas and a centred rarefaction wave travelling into the high pressure gas. In the idealised theory the two gases are separated by a contact surface across which the pressure and velocity are constant but the temperature and density, in general, are not. Using the relationships for changes across shocks and in expansion fans [18] it is possible to construct an analytic theory of the flow until the time at which either the shock or rarefaction wave reaches a boundary. Details of this solution are given in most standard textbooks on gas dynamics (see, for example, [19]).

This system provides an ideal test for our code and indeed the problem has been used extensively in code development. In this paper we use two test problems, specified in references 20 and 21, which were used in the validation of the SIMMER code.

In the first simulation the two gases in the shock tube are the same. The parameters used in the simulation are given in Table 2. This simulation is for a relatively weak shock with gas at 2 MPa expanding into gas at 0.1 MPa producing a shock pressure ratio of 4.24. 96 mesh points and a time-step of 20 $\mu$s were used in the simulation.

Figures 3(a) - 3(d) show a comparison of the computed and exact solutions for the velocity, pressure, density and temperature as a function of distance at 0.02s after the diaphragm has been removed. Figure 3(a) shows that the velocities of the shock wave and the head of

the expansion fan are well predicted and that the calculated velocity is in generally good agreement with the exact solution. There is no overshoot in the velocity behind the shock wave as occurred in the SIMMER calculation. The pressure field is in good agreement with the analytic solution. The density is in generally good agreement with the analytic solution except that the density jump across the contact surface has been smoothed out by numerical diffusion. The temperature profile is very close to the analytic solution showing the characteristic feature of the heating of the gas by the passage of the shock wave and cooling of the gas across the expansion fan.

As a second example we examine the case of a strong shock in a shock tube containing two different gases. The conditions and parameters used in the simulation are given in Table 3. In this case the pressure ratio across the shock was 33.3. Figures 4(a) - 4(d) show a comparison of the computed and the analytic solutions for the velocity, pressure, density and temperature as a function of distance at 0.008s after the diaphragm has been removed. Suitable relaxation rates were chosen to ensure that the velocities and temperatures of the gases were the same in regions where both species were present. It should be noted that the analytic solution assumes that no gas flows across the contact surface whereas in the simulation and in reality the gases will mix. Thus, in contrast to the previous case, the analytic solution is only an approximate model.

Figure 4(a) shows that again the computed velocity field is in good agreement with the analytic solution. The total pressure shown in Figure 4(b) is also in good agreement with the analytic solution and the mixing of the gases is clearly shown. The density and temperature plots are not in such good agreement with the analytic theory because the theory does not allow for the mixing of the gases. However, the agreement is good in regions where only one gas is present. We may conclude that our code has successfully modelled a very strong shock, where velocities of order 2000 m/s are present. This is much greater (by a factor ~ 10) than detonation velocities measured in vapour explosion experiments so we may conclude that the numerical scheme used to solve the equations is certainly adequate for the vapour explosion application.

## 5. Detonations

Detonations have been studied extensively in connection with the rapid combustion of gases. In a detonation a shock wave propagates through an 'unburnt' gas and raises its temperature. If the temperature rise is sufficiently high combustion begins and the gas mixture will be ignited by the shock wave as it moves. Thus combustion is propagated with a supersonic velocity, a process known as detonation. A detailed study of the process of detonation is given in section 121 of reference 22.

From the point of view of simple analytic modelling detonations are very similar to ordinary shocks. The only difference is that energy is added to the system at the detonation front, which is assumed to be very thin. The amount of energy added is determined by the chemistry of the gases involved. In the vapour explosion application the heat addition behind the shock front will depend on how rapidly and finely the melt is fragmented and how well the melt is able to transfer its heat to the coolant.

Detonations are very similar to shock waves in that the jump conditions, which determine conditions across the front, contain a free parameter. For example, if the pressure, temperature and density are known upstream of the shock (in a frame of reference at rest relative to the shock) then the remaining quantities can only be determined if another parameter is specified. In the study of shock waves this is usually the upstream Mach number, which allows the pressure, temperature and density ratios across the shock to be determined. It is well-known that provided the upstream Mach number is greater than unity a solution to the equations exists and the flow downstream of the shock will be subsonic.

The situation is exactly the same in a detonation (where it is assumed that the energy release due to 'combustion' is known). However, in detonations there is often an additional constraint. Consider, for example, the case of a detonation wave moving away from the closed end of a tube. The velocity is zero at the closed end. This can only be achieved if a rarefaction wave separates the detonation wave from the tube end. It is a necessary condition that downstream of the detonation front the

flow velocity is equal to the local sound speed and in this case the detonation can propagate independently of its distance from the closed end of the tube [22]. This condition on the downstream velocity was first put forward as a hypothesis by D.L.Chapman (1899) and E.Jouguet (1905) and has become known as the C-J condition. It should be noted that the C-J condition does not always have to apply but is generally present if the detonation occurs in a bounded domain. Thus given the upstream conditions and the amount of energy released at the detonation front the solution is completely determined. In the next section we will present some sample detonation calculations carried out with the code described in section 3.

## 5.1 Simulation of an Idealised Detonation

In this section we compare the results of a numerical simulation with the analytic theory for an idealised detonation. In an idealised detonation energy is released behind the shock front in a vanishingly thin layer. We have simulated this in the code by adding a specified amount of energy at one grid point and time advancing the solution until a steady-state is found. The parameters used in the simulation are given in Table 4. The simulation results were compared with the exact solution obtained from reference 22. The exact solution is for a detonation satisfying the C-J condition and this solution was used to specify the correct downstream pressure in the simulation.

Figures 5(a) - 5(e) show the computed and analytic steady-state profiles of pressure, density, temperature, velocity and entropy. The figures show that the numerical solution is in very good agreement with the analytic solution. The numerical detonation front is 'smeared' over only two cells and the jumps in quantities such as temperature and density are well predicted in the numerical simulation. The code predicts pressure and entropy rises which are monotonic.

## 5.2 Simulation of an Extended Detonation

In the previous section we examined the case of an idealised detonation where energy is input over only one grid cell. In the vapour

explosion application energy will be input over an extended region. Thus we decided to carry out calculations where the energy was input over an extended region. The same total amount of energy was input as for the previous example but it was added uniformly over a distance of 0.21m, corresponding to 20 cells in a simulation using a total of 96 continuity cells. An analytic solution was obtained by solving the Rankine-Hugoniot equations across each cell.

Figures 6(a) - 6(e) show a comparison of the calculated pressure, density, temperature, velocity and entropy distributions with the analytic solution for a simulation using 96 grid points. The analytic and computed solutions are in good agreement in all cases with only slight differences between them. These differences were shown to be due to grid error and to decrease as the grid was refined by performing simulations with 48, 96 and 192 grid points. These showed that the finite difference solution was converging to the analytic solution. The simulation using only 48 points predicted the correct behaviour and was close to the analytic solution. This shows that the essential behaviour of the system can be determined by using relatively few grid points.

## 6. Discussion

In this paper we have described a compressible flow code which can model the behaviour of two gases. We have shown that a first order accurate finite difference scheme can be constructed in such a manner that shocks and expansion fans are accurately predicted in a thermodynamically consistent manner. This has been achieved by ensuring that the Rankine-Hugoniot equations (in their finite difference form) are built into the finite difference scheme. We have also shown that the code can be used to model detonations and that it also gives accurate results in this situation. In addition the code is very cheap to use. For example, the transient shock tube calculations took less than 10cpu seconds on the Cray XMP.

The present work has been carried out in order to validate a finite difference scheme in situations where there is a known analytic solution.

For this reason we examined a mixture of gases. In the vapour explosion application we are concerned with modelling the propagation of detonations through macroscopic regions of melt, water and steam. This will require the use of a multiphase flow treatment which allows each finite difference cell to contain macroscopic regions of each component, all at a common pressure. The principles developed in this paper will be used to formulate a finite difference scheme to study the behaviour of such systems.

References


1. G.Long, Explosions of molten metals in water, causes and prevention. Metals Progress, 71, 107-112 (1957).
2. D.L.Katz and C.M.Sliepcevich, Liquefied natural gas/water explosions: cause and effect. Hydrocarbon Process, 50, 240-244 (1971).
3. S.A.Colgate and T.Sigurgeirsson, Dynamic mixing of water and lava. Nature, 244, 552-555 (1973).
4. A.W.Cronenberg, Recent developments in the understanding of energetic molten fuel coolant interaction. Nuclear Safety, 21, 319-337 (1980).
5. D.F.Fletcher, A review of coarse mixing models. Culham Laboratory report CLM-R251 (1985).
6. D.F.Fletcher, Assessment and development of the Bankoff and Han coarse mixing model. Culham Laboratory report CLM-R252 (1985).
7. A.Thyagaraja, D.F.Fletcher and I.Cook, One dimensional calculations of two-phase mixing flows. Int. J. Numer. Methods Eng., 24, 459-469 (1987).
8. D.F.Fletcher and A.Thyagaraja, Numerical simulation of one-dimensional multiphase mixing. Culham Laboratory report CLM-P776 (1986).
9. A.Thyagaraja and D.F.Fletcher, Buoyancy-driven, transient, two-dimensional thermo-hydrodynamics of a melt-water-steam mixture. Culham Laboratory report CLM-P790 (1986). (Accepted for publication in Computers and Fluids).
10. D.F.Fletcher and A.Thyagaraja, Numerical simulation of two-dimensional transient multiphase mixing. Paper to be presented at the 5th International Conference on Numerical Methods for Thermal Problems. Montreal, Quebec. June 29 - July 3, 1987. (Also available as Culham Laboratory report CLM-P808.)
11. D.F.Fletcher and A.Thyagaraja, A method of quantitatively describing a multi-component mixture. Paper presented at the 6th International conference on PhysicoChemical Hydrodynamics, Oxford, England, April 8-10, 1987 (Also available as Culham Laboratory report CLM-P812).
12. H.B.Stewart and B.Wendroff, Two-phase flow: Models and methods. J.Comp.Phys., 56, 363-409 (1984).
13. M.W.Zemansky, Heat and Thermodynamics, McGraw-Hill, London. (1968).
14. G.K.Batchelor, An Introduction to Fluid Mechanics, Cambridge University Press, Cambridge. (1967).

15. F.H.Harlow and A.A.Amsden, Numerical calculation of multiphase fluid flow. J.Comp.Phys., 17, 19-52 (1975).

16. G.Moretti, Computation of flows with shocks. In Annual review of fluid mechanics, volume 19. edited by J.L.Lumley, M.Van Dyke and H.L.Read. (1987).

17. A.Thyagaraja, Thermodynamic considerations in the numerical simulation of steady compressible flow. Int. J. Numer. Methods Eng., 15, 437-450 (1980).

18. E.L.Houghton and A.E.Brock, Tables for the compressible flow of dry air. Arnold, London (1970).

19. H.W.Liepmann and A.Roshko, Elements of gas dynamics. Wiley, New York (1960).

20. I.P.Jones and A.V.Jones. The numerical solution of simple one-dimensional multiphase flows in shock tubes. Paper presented at the 2nd International Conference on Numerical Methods in Laminar and Turbulent Flow, Venice, July 13-16, 1981. (Also available as Harwell Laboratory Report CSS99).

21. P.J.Blewitt, SIMMER-II, calculation of shock tube problems. NUREG/CR-0385. (1978).

22. L.D.Landau and E.M.Lifshitz, Fluid Mechanics. Pergamon Press, Oxford. (1982).

| | |
|---|---|
| Solution domain length | 1m |
| Number of grid points | 72 |
| Upstream pressure | $1.2 \times 10^5$ N/m$^2$ |
| Upstream density | 1 kg/m$^3$ |
| Upstream temperature | 400 K |
| Upstream Mach Number | 2 |
| Downstream Pressure | $5.631 \times 10^5$ N/m$^2$ |
| $c_v$ | 300 J/kgK |
| $\gamma$ | 1.6 |

Table 1: Parameters used in the stationary shock calculation

High pressure section

| | | |
|---|---|---|
| $p$ | = | 2 MPa |
| $\rho$ | = | 10.7 kg/m$^3$ |
| $T$ | = | 413.86K |
| $\gamma$ | = | 4/3 |
| $c_v$ | = | 1355 J/kgK |

Low pressure section

| | | |
|---|---|---|
| $p$ | = | 0.1MPa |
| $\rho$ | = | 0.738 kg/m$^3$ |
| $T$ | = | 300K |
| $\gamma$ | = | 4/3 |
| $c_v$ | = | 1355 J/kgK |

General parameters

| | | |
|---|---|---|
| Length of shock tube | = | 44m |
| Position of Diaphragm | = | 22m |
| Comparison time | = | 0.02s |
| Number of grid points | = | 96 |
| Time-step | = | 20 μs |

Table 2: Parameters for the weak shock simulation

High pressure section

| | | |
|---|---|---|
| $p$ | = | 20 MPa |
| $\rho$ | = | $10.7 kg/m^3$ |
| $T$ | = | 413.86K |
| $\gamma$ | = | 4/3 |
| $c_v$ | = | 13550 J/kgK |

Low pressure section

| | | |
|---|---|---|
| $p$ | = | 0.1MPa |
| $\rho$ | = | $0.738 kg/m^3$ |
| $T$ | = | 300K |
| $\gamma$ | = | 4/3 |
| $c_v$ | = | 1355 J/kgK |

General parameters

| | | |
|---|---|---|
| Length of shock tube | = | 44m |
| Position of diaphragm | = | 14.6m |
| Comparison time | = | 0.008s |
| Number of grid points | = | 96 |
| Time-step | = | 5 $\mu$s |

Table 3: Parameters for the strong shock simulation

Unburnt Gas

$p = 10^5$ N/m$^2$

$\rho = 0.6$ kg/m$^3$

$T = 417$K

$v = 4382$ m/s

$\gamma = 1.4$

$c_v = 1000$ J/kgK

Burnt Gas

$\gamma$ and $c_v$ the same as for the unburnt gas

$10^7$ J/kg released upon burning the gas

Downstream pressure = 4.95 MPa

Detonation satisfies C-J condition

General Parameters

| | | |
|---|---|---|
| Solution domain length | = | 1m |
| Number of grid points | = | 48 |
| Time-step | = | 0.5μs. |

Table 4: Parameters for the Idealised Detonation Simulation

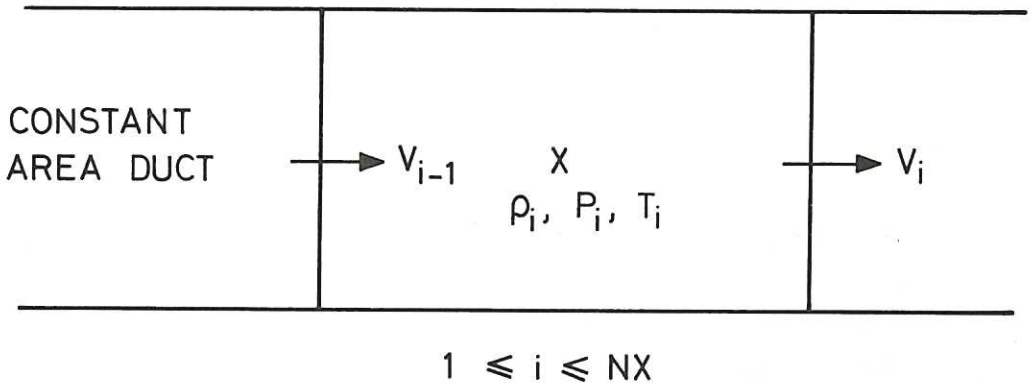


Fig. 1 A Typical Finite Difference Cell.

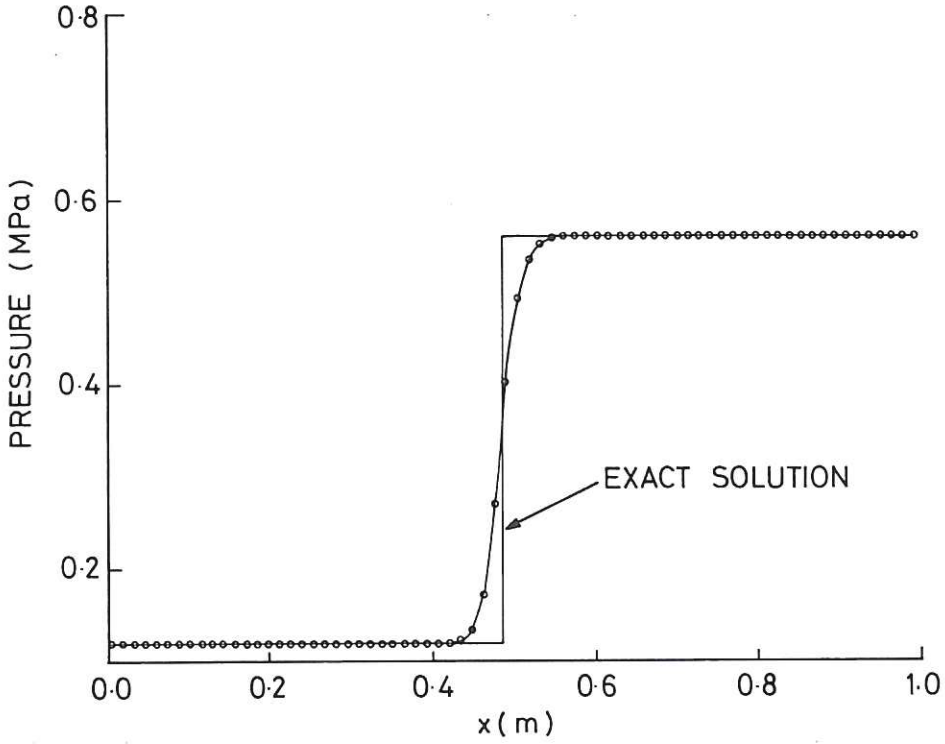


Fig. 2(a) Pressure Profile for the Steady Shock Calculation

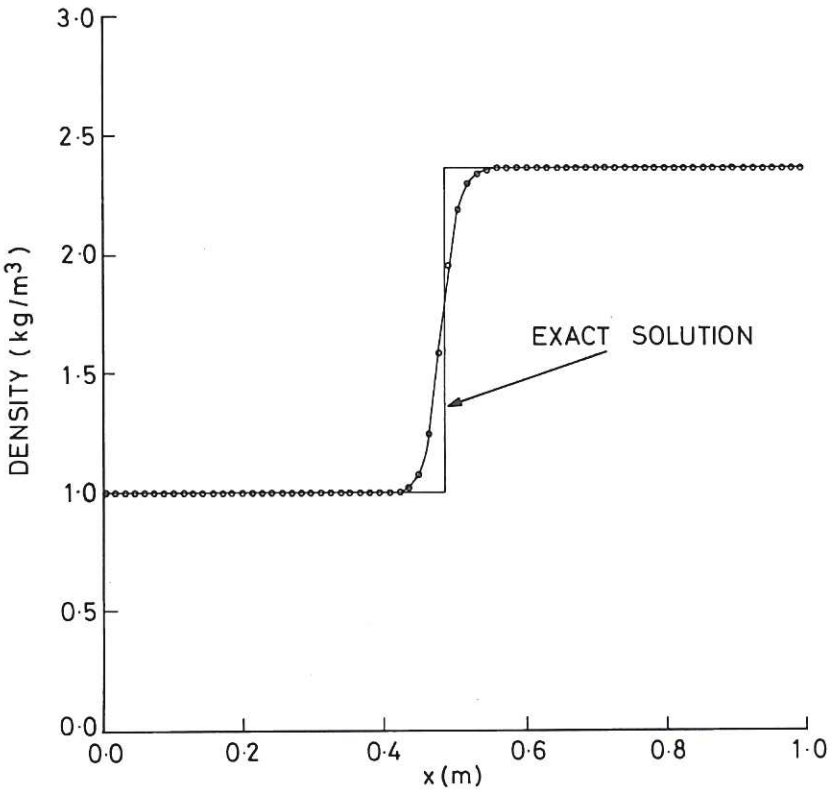


Fig. 2(b) Density Profile for the Steady Shock Calculation

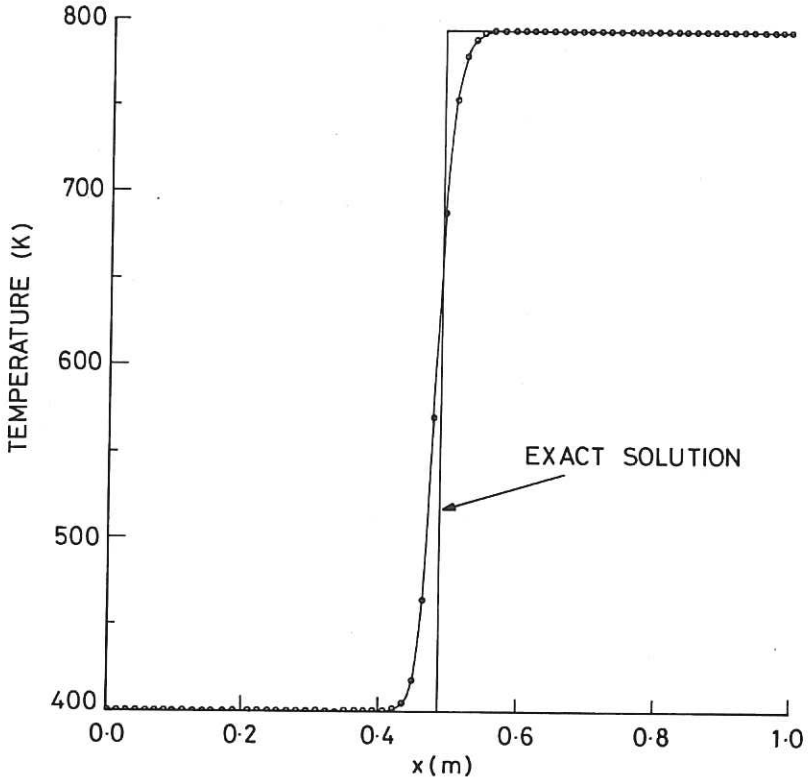


Fig. 2(c) Temperature Profile for the Steady Shock Calculation.

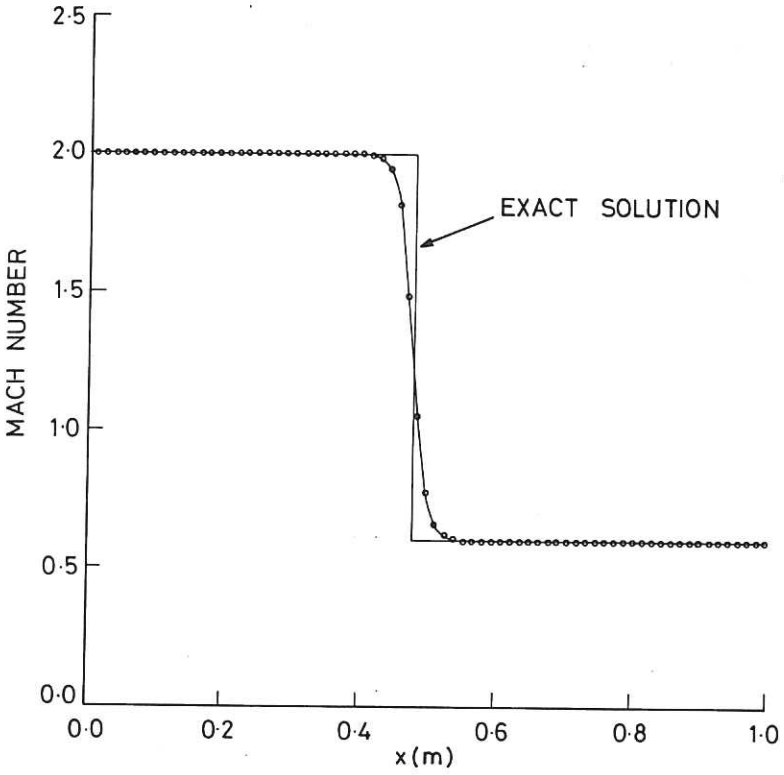


Fig. 2(d) Mach Number Profile for the Steady Shock Calculation

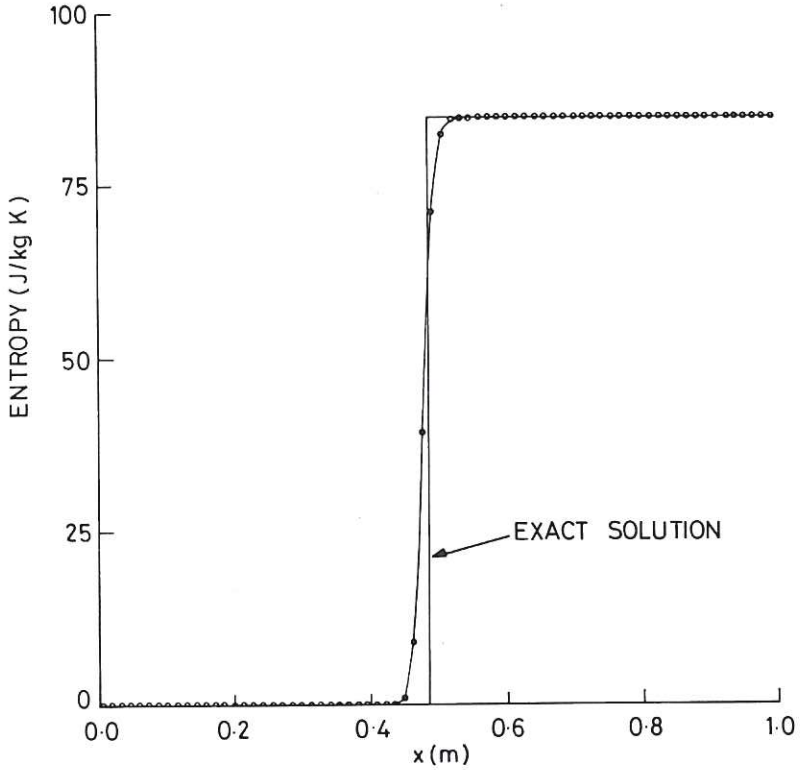


Fig. 2(e) Entropy Profile for the Steady Shock Calculation

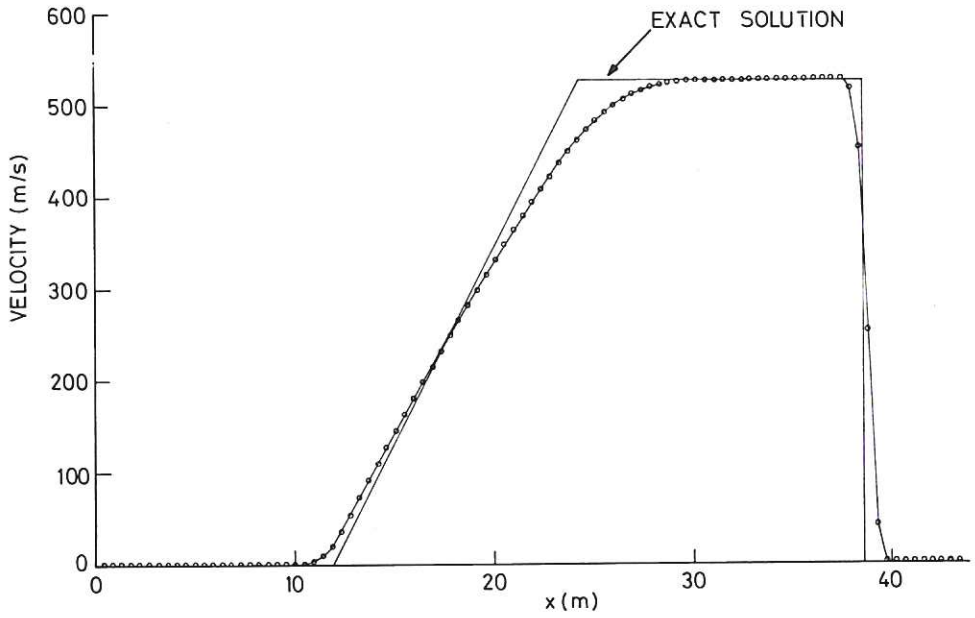


Fig. 3(a) Weak Shock Simulation, Velocity as a Function of Distance after 0.02 s

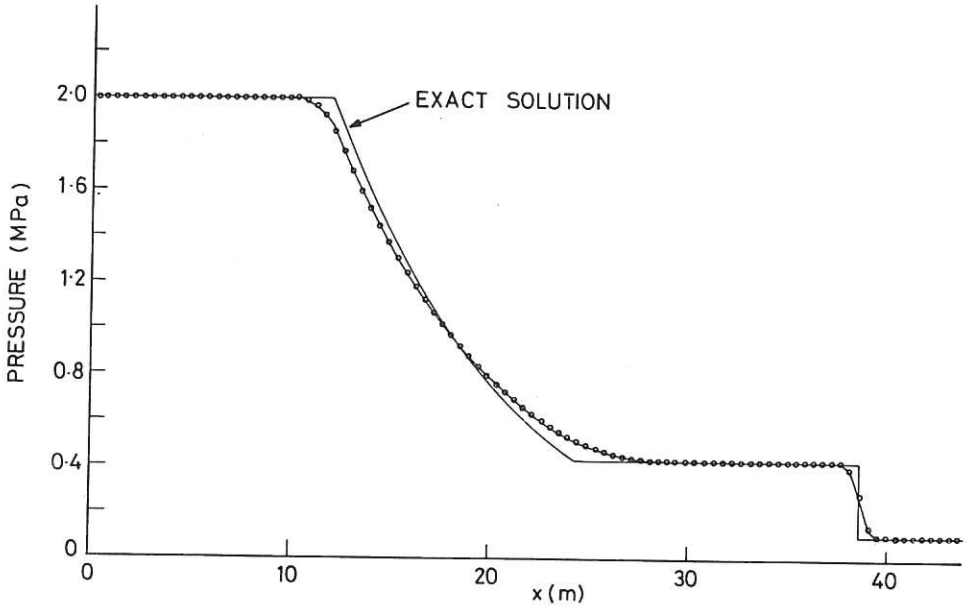


Fig. 3(b) Weak Shock Simulation, Pressure as a Function of Distance after 0.02s

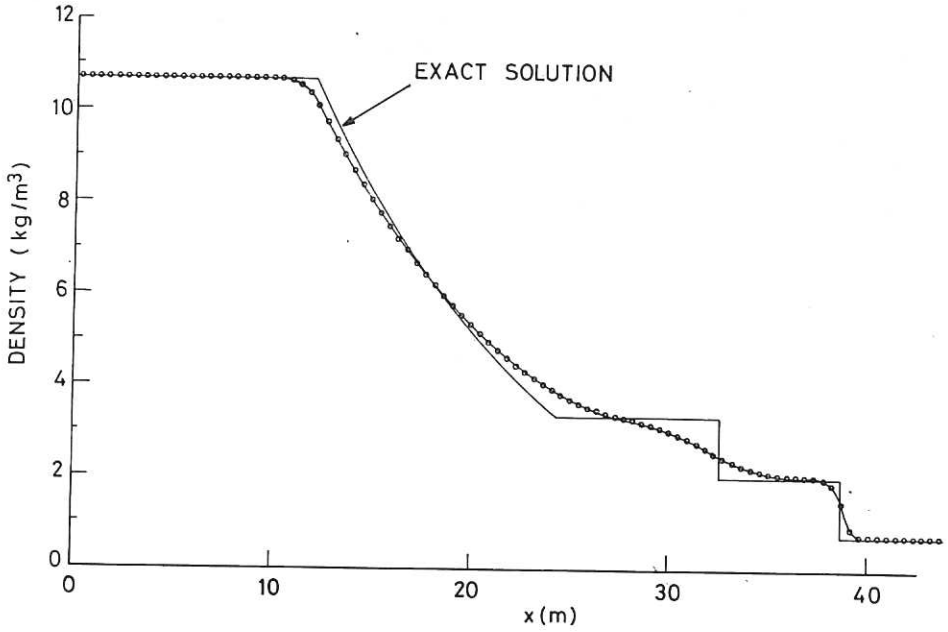


Fig. 3(c) Weak Shock Simulation, Density as a Function of Distance after 0.02s

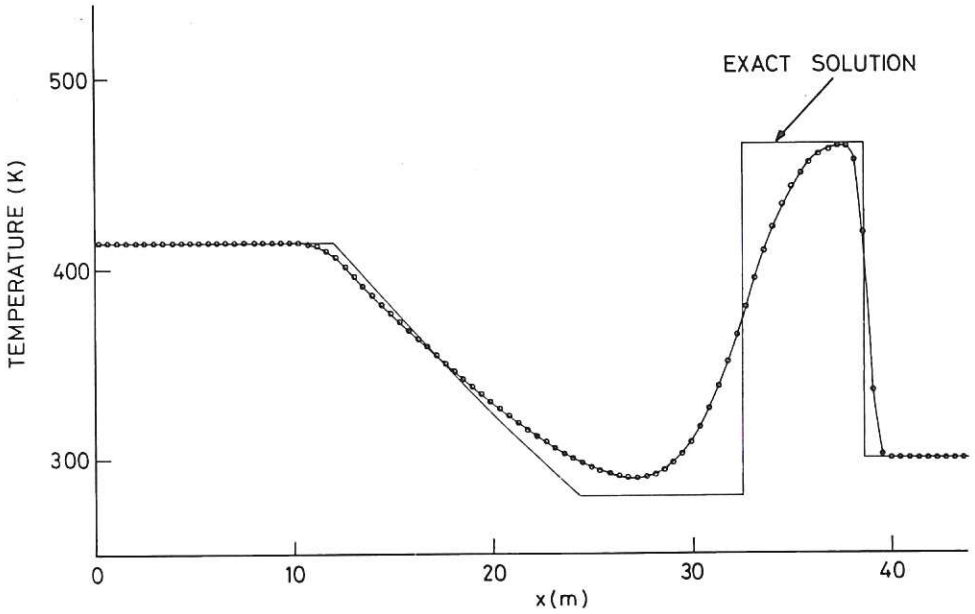


Fig. 3(d) Weak Shock Simulation, Temperature as a Function of Distance after 0.02s

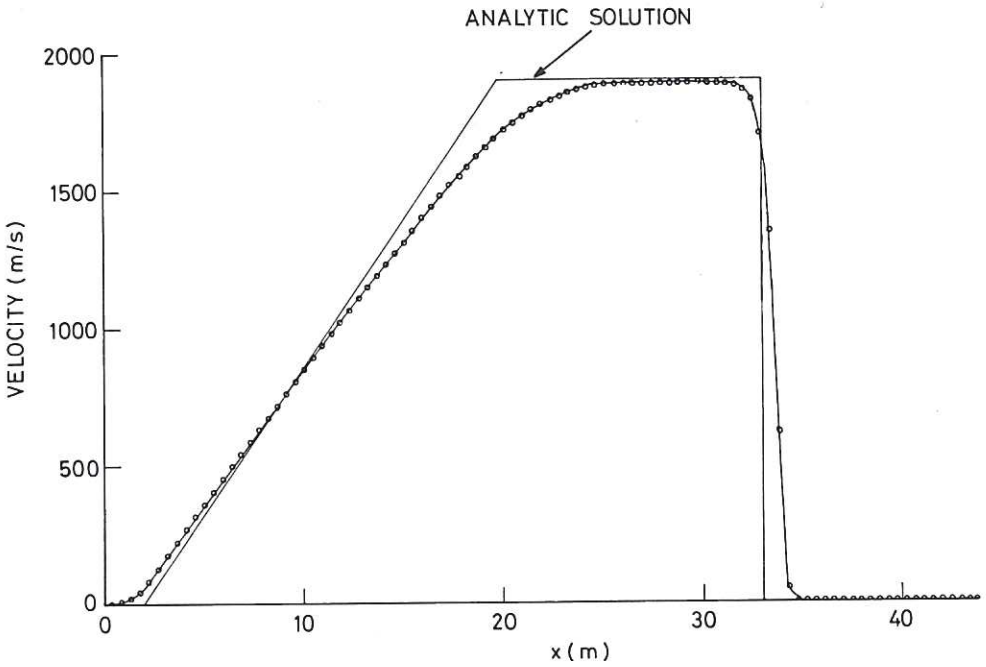


Fig. 4(a) Strong Shock Simulation, Velocity as a Function of Distance after 0.008s

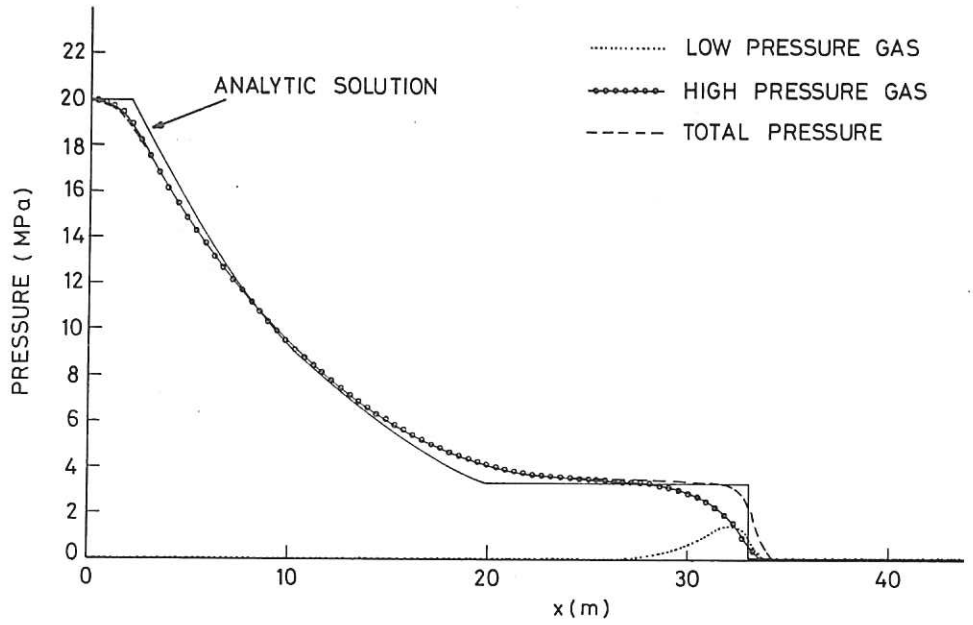


Fig. 4(b) Strong Shock Simulation, Pressure as a Function of Distance after 0.008 s.

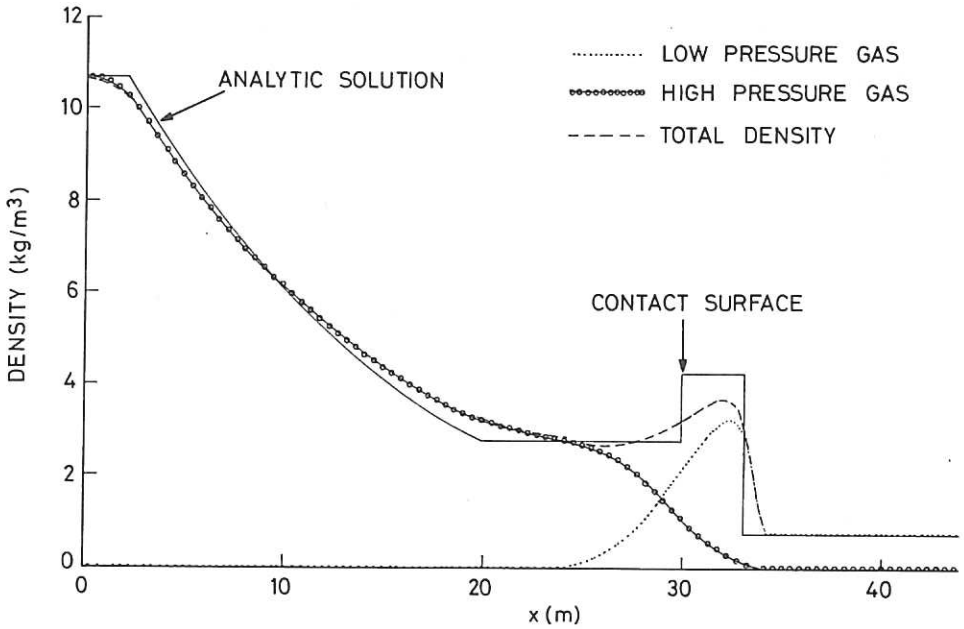


Fig. 4(c) Strong Shock Simulation, Density as a Function of Distance after 0.008 s

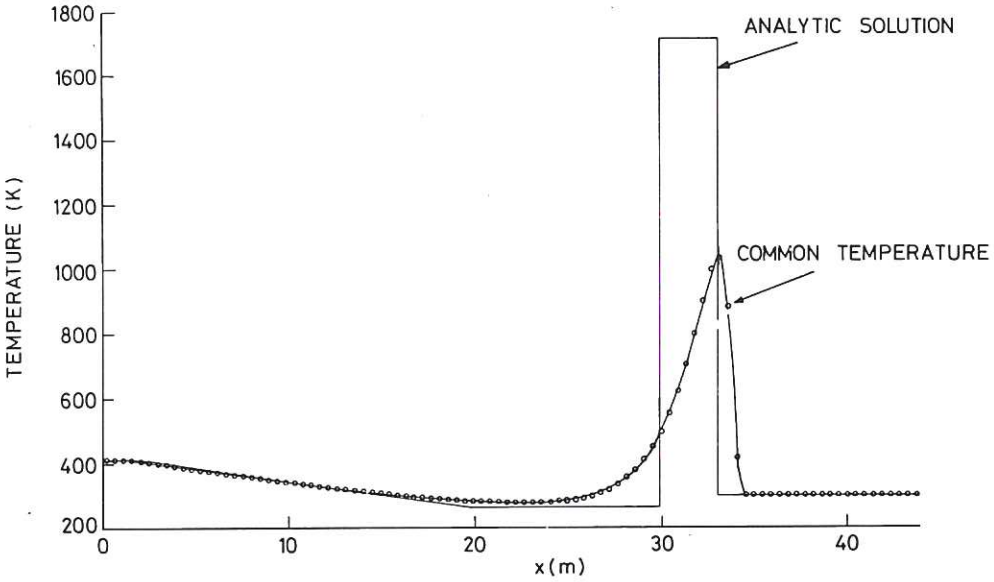


Fig. 4(d) Strong Shock Simulation, Temperature as a Function of Distance after 0.008 s

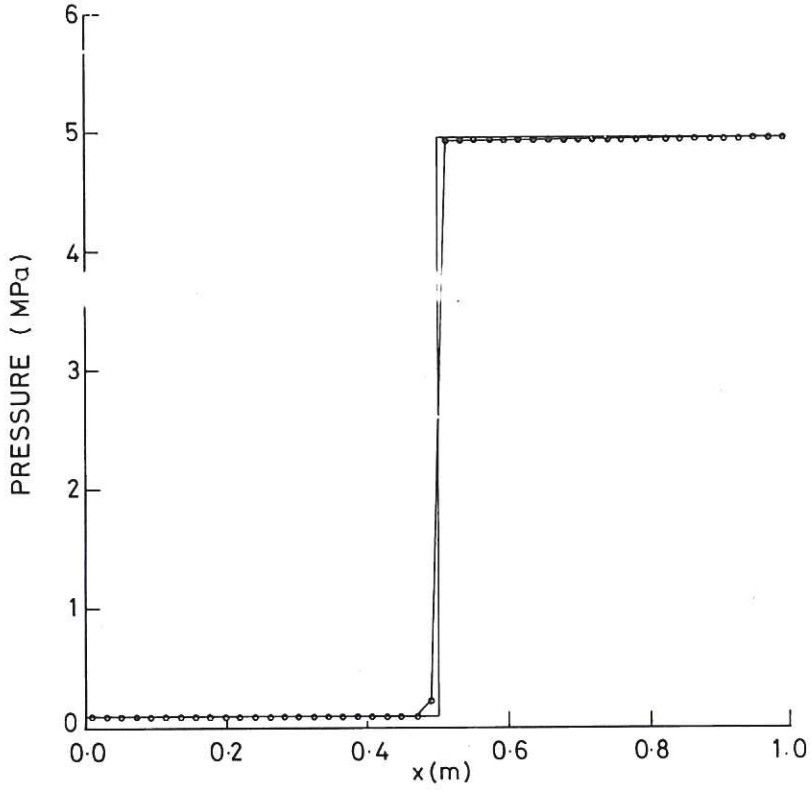


Fig. 5(a) Pressure Profile for the Idealised Detonation Simulation

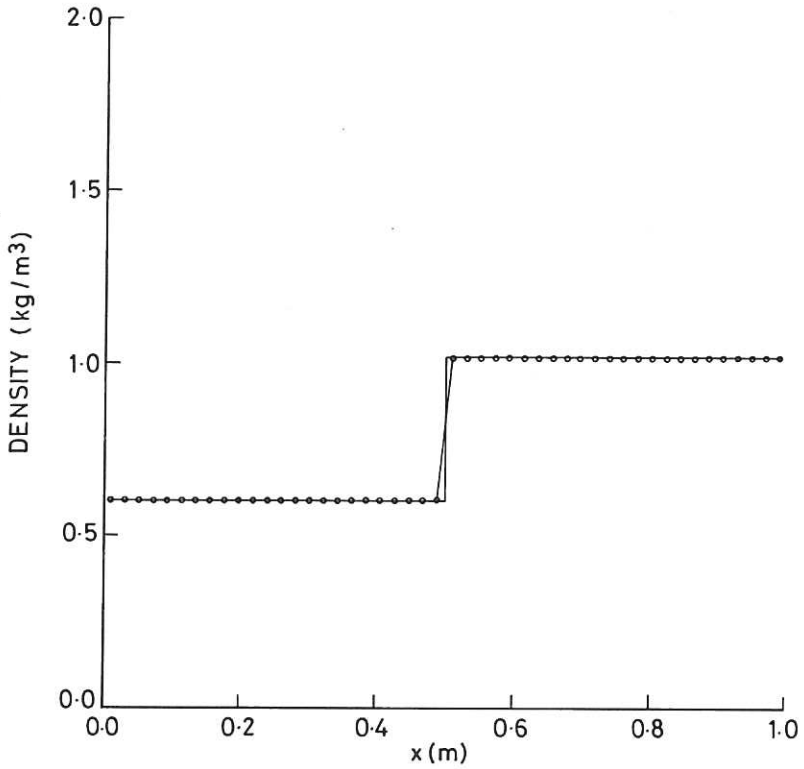


Fig. 5(b) Density Profile for the Idealised Detonation Simulation

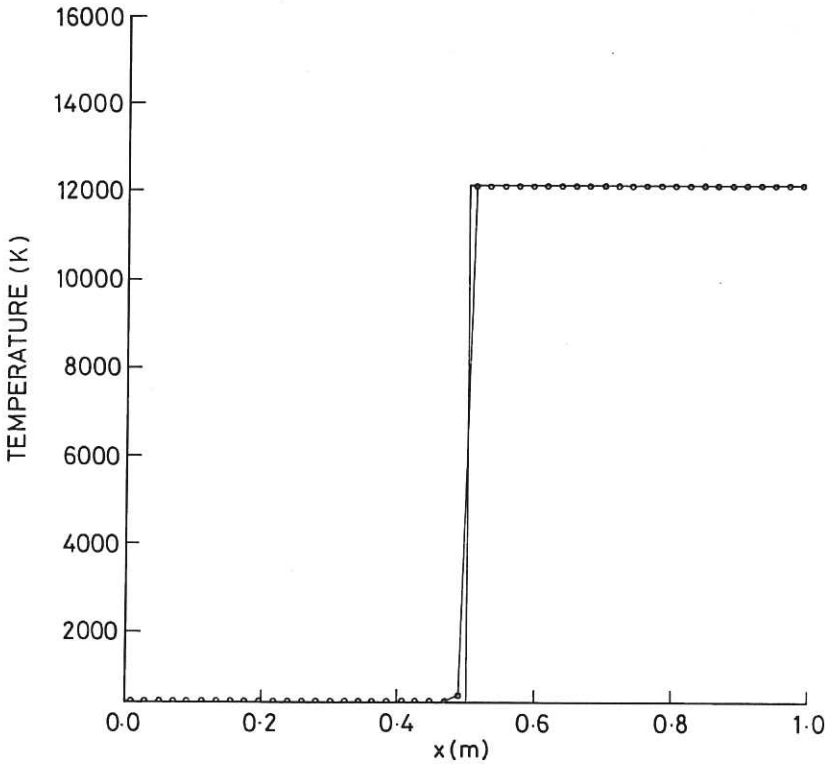


Fig. 5(c) Temperature Profile for the Idealised Detonation Simulation.

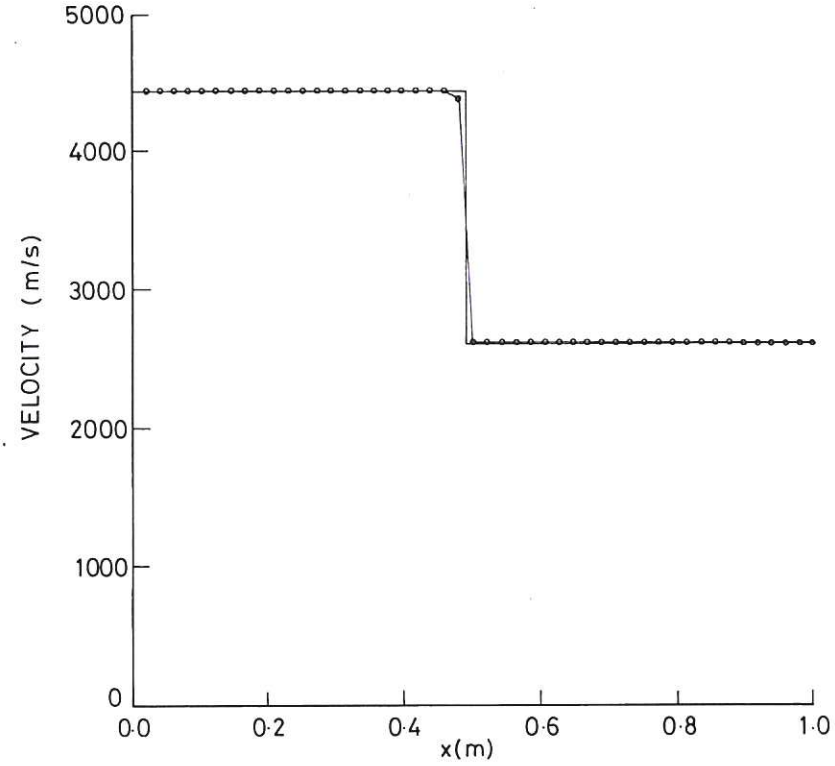


Fig. 5(d) Velocity Profile for the Idealised Detonation Simulation

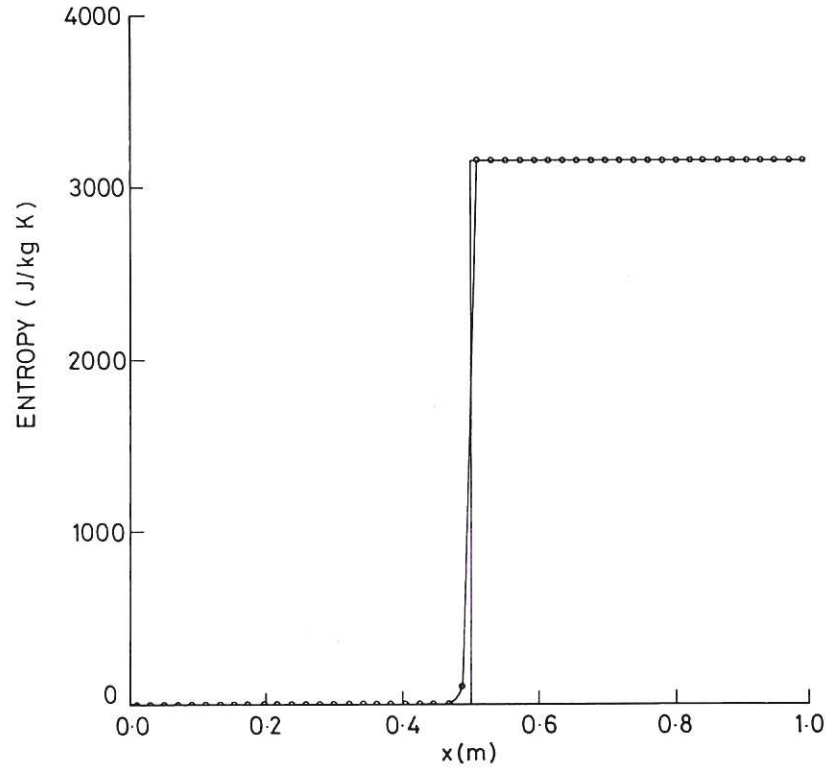


Fig. 5(e) Entropy Profile for the Idealised Detonation Simulation

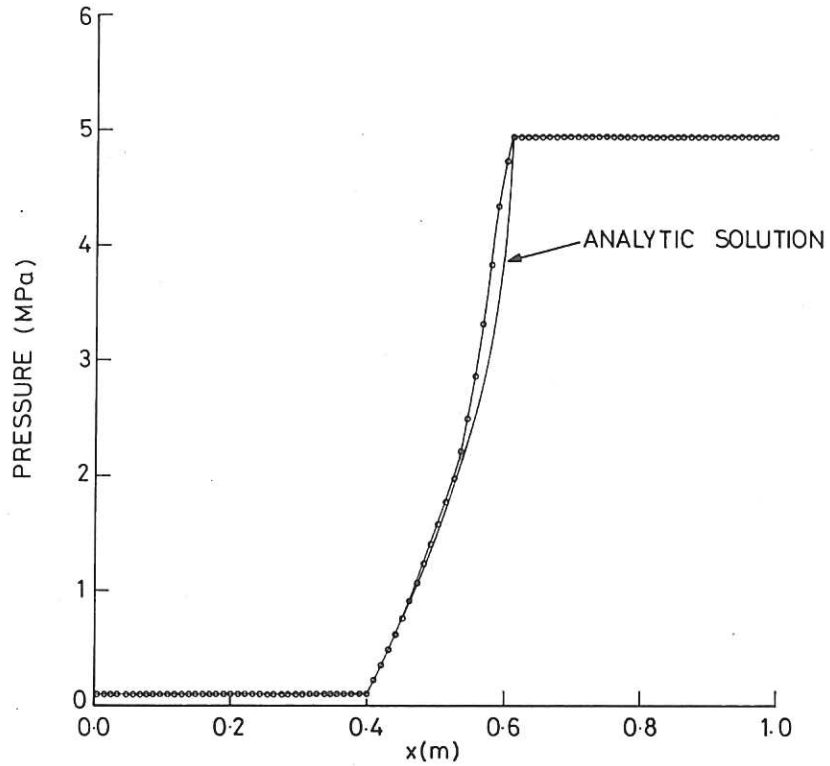


Fig. 6(a) Pressure Profile for the Extended Detonation Simulation

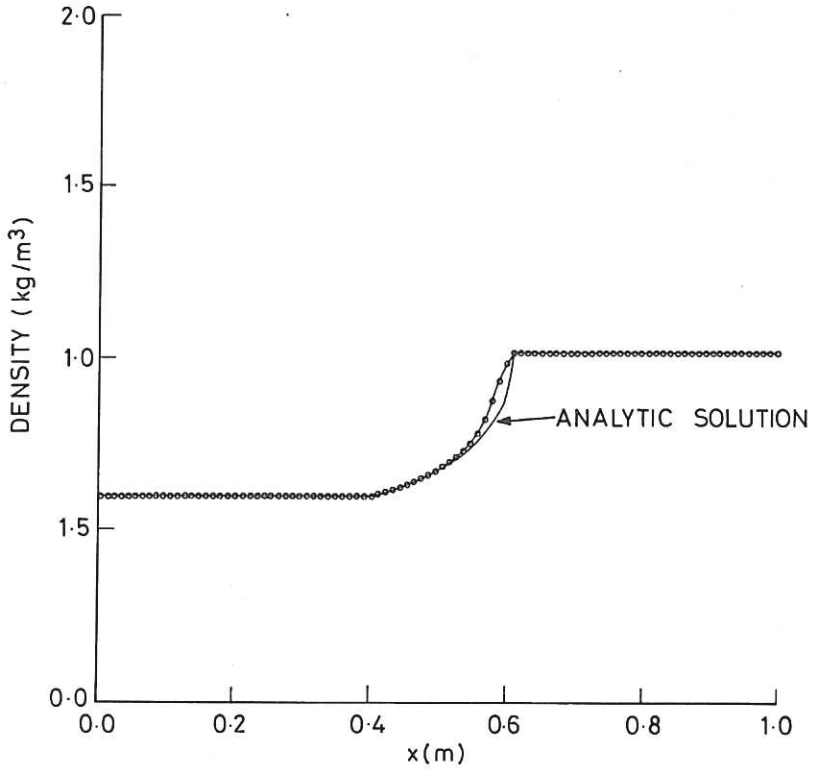


Fig. 6(b) Density Profile for the Extended Detonation Solution

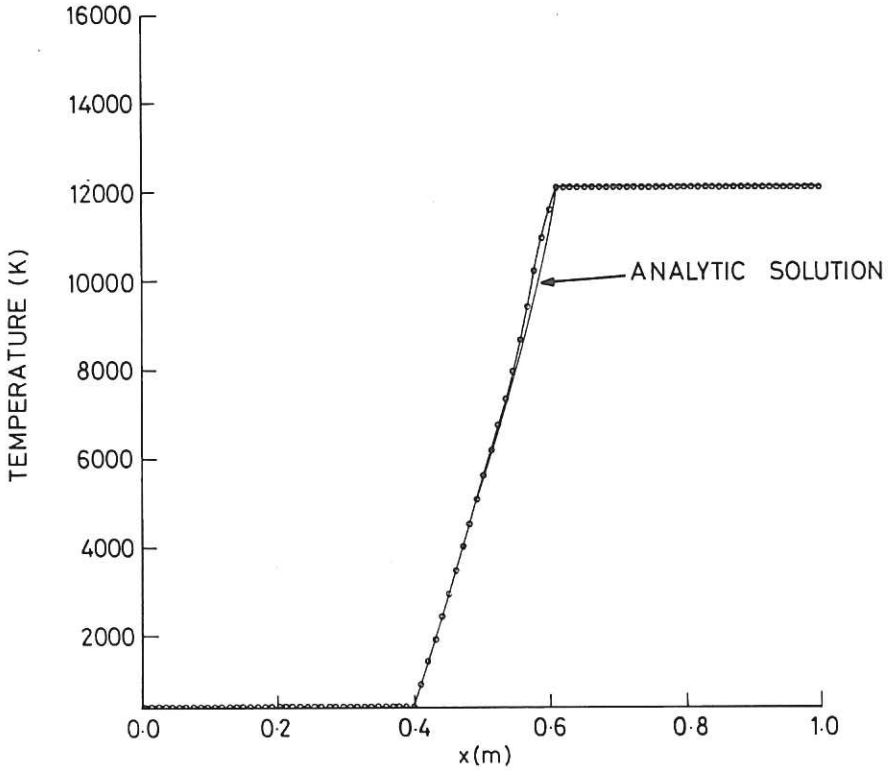


Fig. 6(c) Temperature Profile for the Extended Detonation Simulation

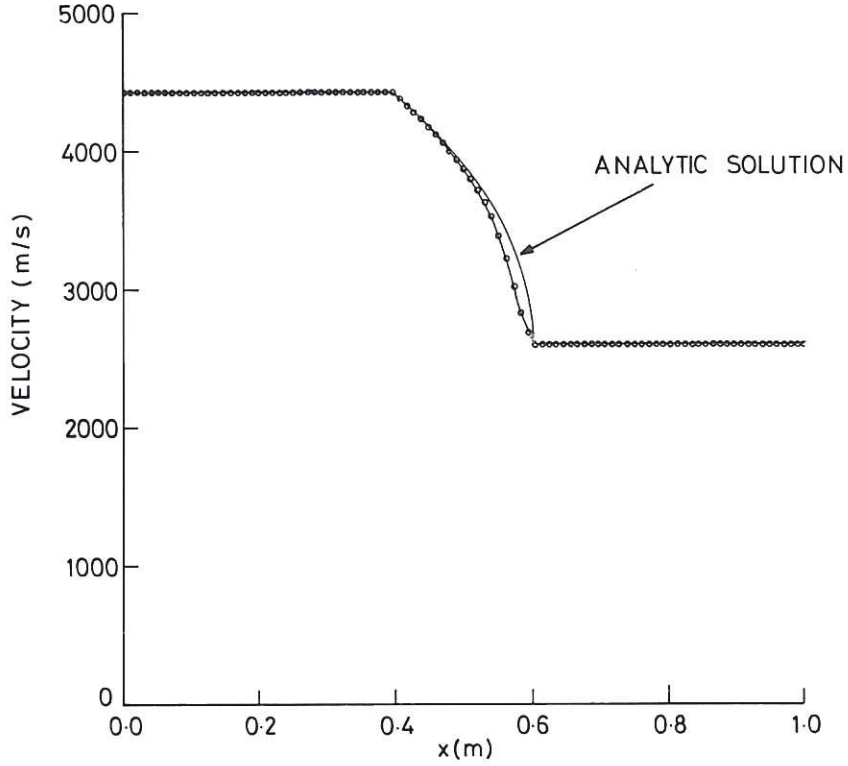


Fig. 6(d) Velocity Profile for the Extended Detonation Simulation

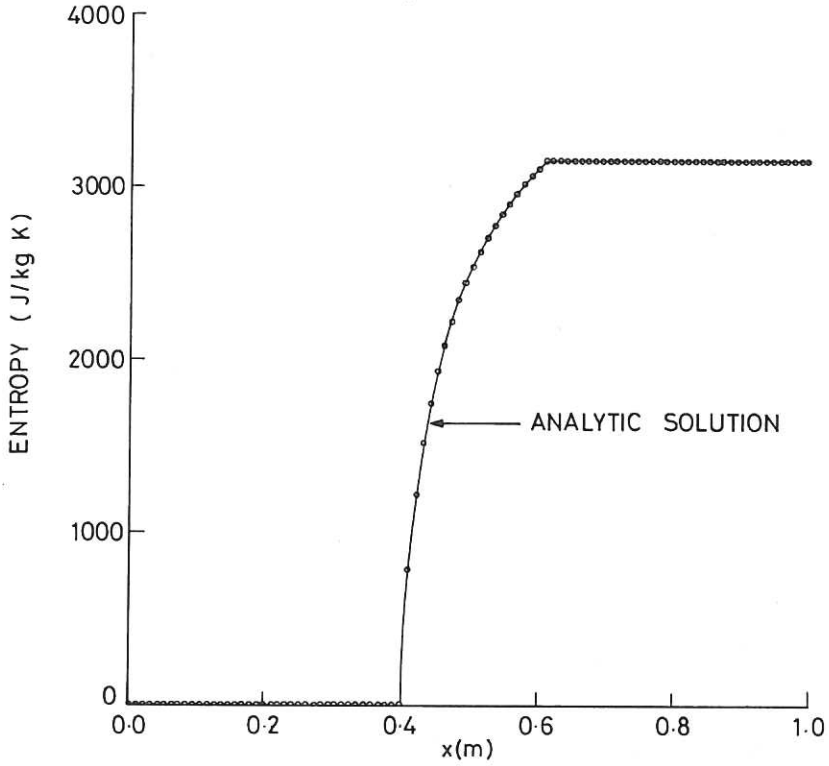


Fig. 6(e) Entropy Profile for the Extended Detonation Simulation.